16 EFFECT OF SURFACE EXCHANGE COEFFICIENTS ON THE DEVELOPMENT OF INNER-CORE ASYMMETRIES IN SIMULATED TROPICAL CYCLONES

Jason Naylor* and David Schecter
NorthWest Research Associates, Boulder, CO

1. INTRODUCTION

Strong tropical cyclones are often characterized by non-monotonic radial profiles of potential vorticity (PV). Basic theory suggests that such profiles can be unstable, resulting in PV mixing and the development of eyewall mesovortices (e.g. Schubert et al. 1999, Kossin and Schubert 2001, Nolan and Montgomery 2001, Schecter and Montgomery 2007, Rozoff et al. 2009). However, the actual conditions for eyewall instability and the full consequences of instability on tropical cyclone intensity are topics of ongoing research.

The purpose of this study is to investigate how variations in the surface exchange coefficients of enthalpy (c_e) and momentum (c_d) influence the type of asymmetry that develops in moist, 3D tropical cyclone simulations and to examine the intensity change associated with the development of these asymmetries. In addition, dry 3D simulations have been conducted to gain insight into how the removal of the moist secondary circulation may affect asymmetry development.

2. METHODOLOGY

Simulations were completed using version 16 of CM1 (www.mmm.ucar.edu/people/bryan/cm1). The domain was 2122.5 km x 2122.5 km x 30 km. The horizontal grid had constant 250 m grid spacing over a distance of 175 km in the center of the domain. Beyond this point, grid spacing gradually increased to 10 km. In the vertical, a constant grid spacing of 100 m was used in the lowest 3 km. Above this level, the grid spacing gradually increased to 500 m.

Precipitation processes were represented by a simple, 3-class (water vapor, cloud water, rain) warm rain microphysics parameterization. Subgrid turbulence was parameterized using a first-order closure scheme in which the eddy viscosity is proportional to the flow deformation (iturb=3 option in the cm1 namelist). The horizontal mixing length was defined to be 250 m, whereas the vertical mixing length was height dependent and approached a value of 200 m. A relaxation term of 2 K day^{-1} was applied to the potential temperature field to approximate radiative cooling (cf. Rotunno and Emanuel 1987). The horizontally homogenous background was initialized with the moist tropical sounding from Dunion (2011) and a constant sea surface temperature of 299.15 K. Surface exchange processes were represented with constant values (both in time and space) of c_e and c_d. Three simulations are presented herein: c_e/c_d=0.5 with c_e=0.0015, c_e/c_d=0.5 with c_e=0.003, and c_e/c_d=1 with c_e=0.0015.

Before the 3D simulations were carried out, axisymmetric simulations were performed. These simulations used the same configuration as the 3D simulations, except with half the horizontal domain. In the axisymmetric simulations, the initial vortex was that of Rotunno and Emanuel (1987). These simulations were run for 18 days. A time average was taken once the simulations reached a quasi steady-state. The 3D simulations were initialized with this time-averaged state after conversion to Cartesian coordinates and addition of pseudo-random potential temperature perturbations.

3. RESULTS

The steady-state, time-averaged profiles of PV from the 2D simulations are shown in Fig. 1. Each simulation exhibits a strong, PV ‘ring’ at z=1.2 km, with a weak secondary PV peak just beyond the main PV ring. The sharpest ring occurs in the simulation with c_e/c_d =0.5 and c_e=0.003. Above z=1.2 km, the radial PV profiles differ between simulations. In the c_e/c_d =0.5 simulations, there are multiple altitudes where PV increases with radius from r=0 km to r~15 km, whereas the c_e/c_d =1 simulation exhibits more of a monopole structure, with PV being relatively constant, or even decreasing, with radius.

3.1 *Moist 3D Simulations*

The most noticeable asymmetry occurs in the simulation with c_e/c_d =0.5 and c_e=0.0015 (Fig 2, left panel). By t=6 hrs, the vertical vorticity field has developed an elliptical shape that persists for the duration of the simulation. Similar elliptical shapes are seen in the other two simulations (Figs. 2, middle and right panels), however they are less pronounced.

* *Corresponding author address*: Jason Naylor, NorthWest Research Associates, 3380 Mitchell Lane, Boulder, CO, 80301. Email: jnaylor@nwra.com

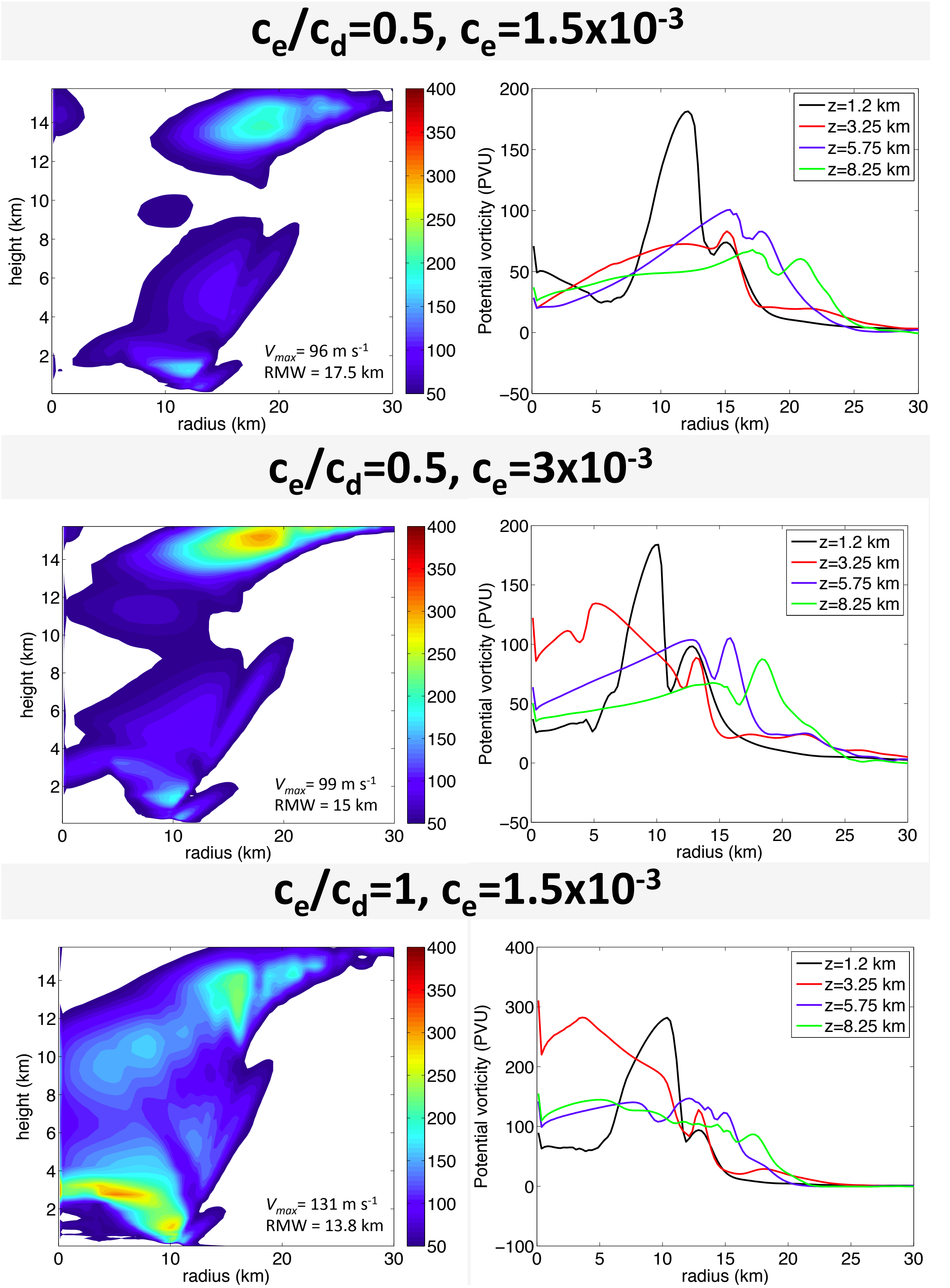

FIG 1. Steady-state, time-averaged profiles of potential vorticity from the axisymmetric simulations. Left column shows height-radius cross sections, and the right panel shows radial profiles at selected heights. The maximum wind speed (V_{max}) and radius of maximum wind (RMW) are shown for each simulation.

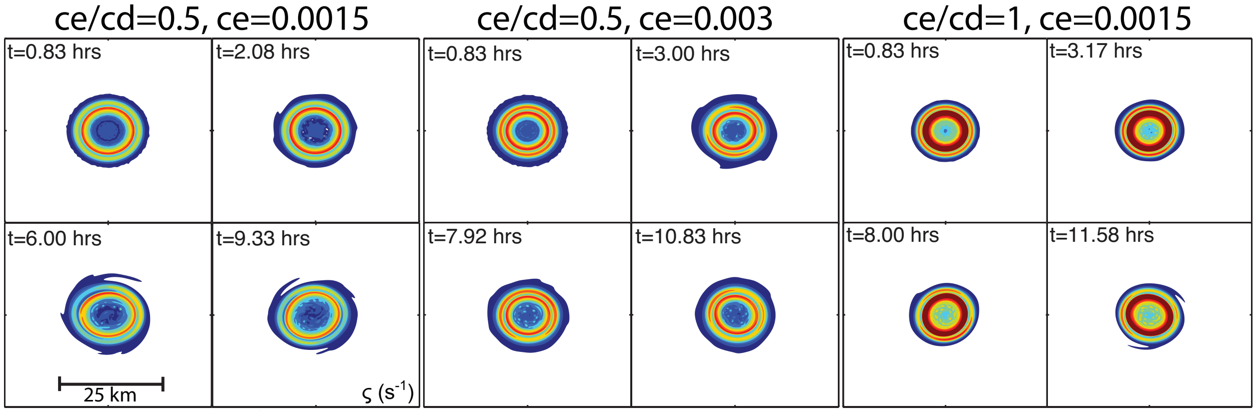

FIG. 2. Overview of vertical vorticity evolution at z=1.2 km. Contours range from 0.002 s^{-1} (dark blue) to 0.02 s^{-1} (dark red).

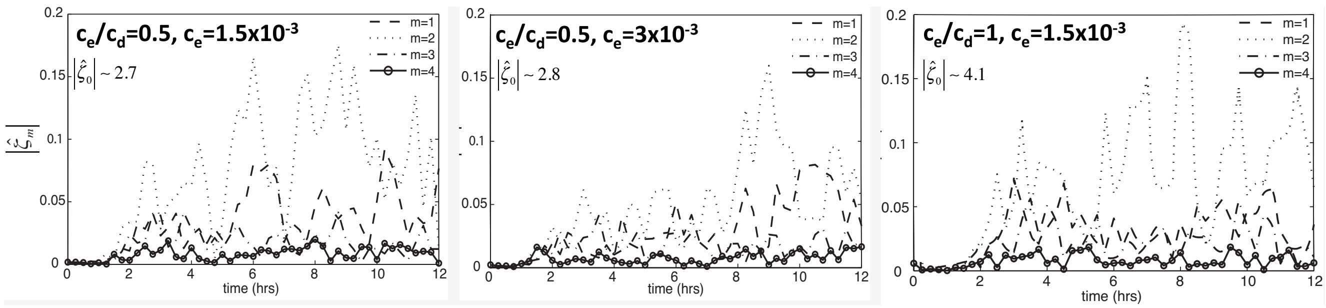

FIG. 3. Time series of Fourier amplitudes of vertical vorticity for azimuthal wavenumbers 1-4. The Fourier analysis is performed on vertical vorticity averaged from z=1 km to z=5 km and over a 2 km radial interval centered on the RMW. The magnitude of the symmetric component of vorticity (i.e. wavenumber 0) is shown in each panel. Units are s^{-1}.

Somewhat surprisingly, none of the moist simulations appear to experience eyewall breakdown or the development of mesovortices. A closer examination of the inner-core asymmetries was done via a Fourier analysis of vertical vorticity (ζ):

$$\hat{\zeta}_m = \sum_{j=0}^{N-1} \zeta(j) e^{i2\pi mj/N} , \qquad (1)$$

where j is the azimuth in degrees, N=360, and m is the azimuthal wavenumber. The decomposition used ζ averaged over a 2 km radial interval centered on the radius of maximum wind (RMW) and also averaged over a vertical depth ranging from z=1 km to z=5 km.

In all three simulations, the dominant asymmetry is wavenumber-2, followed by wavenumber-1 (Fig. 3). Note that increasing the magnitude of the surface exchange coefficients by a factor of 2 (while keeping the ratio constant at 0.5) results in a much shorter-lived peak in the wavenumber-2 asymmetry (Fig. 3, middle panel) compared to the simulation with smaller magnitude exchange coefficients (Fig. 3, left panel).

At first glance, Fig. 3 seems to indicate that the Fourier amplitudes have a similar magnitude in all three simulations. However, the symmetric component of vertical vorticity, $|\hat{\zeta}_0|$, in the simulation with c_e/c_d =1 is about 35% larger than that in the simulations with c_e/c_d =0.5. Thus, although the *absolute* magnitude of the asymmetries is similar, the peak magnitude *relative* to $|\hat{\zeta}_0|$ is smaller in the simulation with c_e/c_d =1.

3.2 *Effect of Asymmetries on Maximum Intensity and 'Potential Intensity'*

Next, the evolution of maximum (azimuthally averaged) tangential velocity (V_{max}) and potential intensity is examined. For this analysis, potential intensity is defined using the EPI+ equation from Bryan and Rotunno (2009), which is based on the potential intensity theory originally derived by Emanuel (1986), but includes the effects of unbalanced flow.

The equation for EPI+ is

$$\left(EPI+\right)^2 = \frac{T_s}{T_o}\left[\frac{c_e}{c_d}\left(T_b - T_o\right)\left(s_{sfc} - s_o\right) + r_b \eta_b w_b\right], \quad (2)$$

where T_s is the sea surface temperature, T_o is the outflow temperature, T_b is the temperature at the top of the boundary layer, s_{sfc} is the saturated moist entropy at the sea surface, s_0 is the moist entropy at the top of the surface layer, w_b is vertical velocity, and η_b is azimuthal vorticity. All terms are azimuthal averages (or constants). Terms with a '*b*' subscript are evaluated at the *r*,*z* location of V_{max}. Entropies are evaluated at the RMW and are calculated using the approximate pseudoadiabatic formula from Bryan (2008). The first term on the RHS of (2) represents the gradient wind balance portion of potential intensity (Emanuel 1995; herein also referred to as EPI) and the second term represents the contribution from unbalanced flow.

Figure 4 shows that V_{max} decreases with time in all three simulations. Additionally, the decreases in V_{max} are closely mirrored by decreases in EPI+. However, the gradient balance portion of EPI+ remains relatively constant with time, suggesting that intensity changes associated with asymmetry development coincide with a reduction of imbalance in the mean flow. Also of note is that the simulation that produced the largest asymmetry (c_e/c_d =0.5, c_e=0.0015) experiences the largest decrease in V_{max} and EPI+ (Fig. 4, top panel).

To determine if the decrease in intensity continues past *t*=12 hrs, the simulation with c_e/c_d =0.5,and c_e=0.0015 was extended to *t*=24 hrs (not shown). By *t*=24 hrs, V_{max} and EPI+ have decreased by approximately 8 m s^{-1} (relative to their value at *t*=0 hrs), while EPI has decreased by 2 m s^{-1}. However, the vortex has not quite reached a steady state by *t*=24 hrs (V_{max} decreases by 3.6 m s^{-1} between 18 – 22 hrs). In order to quantify the total intensity change following asymmetric eyewall instability, future work will involve extending all 3D simulations until a quasi-steady state is clearly achieved.

3.3 *Dry Simulations*

Finally, dry 3D simulations were performed in order to evaluate the validity of using dry theory to characterize the development of asymmetries in moist simulations (not shown). Like the moist simulations, the dry, 3D simulations were initialized with the steady-state profiles from the

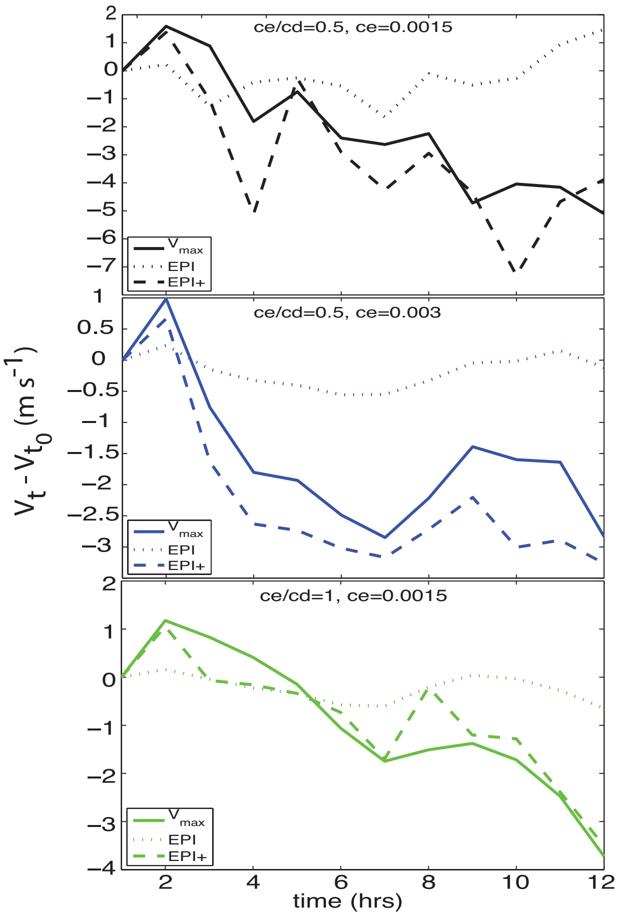

FIG 4. Time series of changes in maximum azimuthally averaged tangential velocity (solid line), EPI+ (dashed line), and the gradient balance portion of EPI+ (EPI, dotted line).

axisymmetric simulations. However, for the dry simulations, only the azimuthal velocity was used in the initialization process. Radial and vertical velocities were set to zero (i.e. the secondary circulation was removed) and the pressure and temperature fields were solved iteratively so that they satisfied thermal wind balance. In addition, surface processes were turned off and the radiative cooling was removed.

All three dry simulations produced asymmetries that developed more rapidly than their moist counterparts. In the dry simulations initialized with the azimuthal wind from the axisymmetric c_e/c_d=0.5 simulations, larger wavenumber asymmetries (m=4 and m=5) were found to dominate (compared to the moist simulations). Conversely, both the moist simulation with c_e/c_d=1 and its dry counterpart were dominated by a wavenumber-2 asymmetry.

Several slight variations of the initialization process for the dry simulations were tested, with all producing similar results. Also, a dry, barotropic stability analysis (cf. Schubert et al.

1999) was performed on the steady-state vertical vorticity profiles from the axisymmetric simulations (i.e. the initial conditions of the dry simulations). When only the low-level (z < 1 km) vorticity structure was considered, the stability analysis was qualitatively consistent with the results from the dry 3D simulations. That is, the moist simulations with c_e/c_d=0.5 are more stable and produce smaller wavenumber asymmetries than expected from the stability analysis or observed in the dry simulations.

4. SUMMARY OF PRELIMINARY FINDINGS

The simulations presented herein have shown how modifying the ratio of surface exchange coefficients, or their magnitudes, can alter the radial PV profile and the stability of three-dimensional hurricane-like vortices. The development of asymmetries in the moist simulations coincided with quantitatively consistent decreases in V_{max} and EPI+. All three moist simulations were dominated by a wavenumber-2 perturbation that began developing after approximately 2 hrs of run time.

Preliminary results from dry simulations revealed that asymmetries developed faster and were often dominated by larger wavenumber features compared to their moist counterparts. This suggests that processes related to the moist secondary circulation can stabilize the vortex and that the use of dry theory may be insufficient for interpreting the growth of asymmetries in tropical cyclones.

ACKNOWLEDGEMENTS

This work is sponsored by NSF grant AGS-1101713. Simulations were performed at the San Diego Supercomputer Center under XSEDE allocation TG-ATM130028. Much of the analysis was completed on NCAR's Geyser cluster, using allocation UNWR0001. We would also like to thank Dr. George Bryan for maintaining CM1 and making it available to the research community.

REFERENCES

Bryan, G. H. 2008: On the computation of pseudoadiabatic entropy and equivalent potential temperature. *Mon. Wea. Rev.*, **136**, 5239-5245.

____. and R. Rotunno, 2009: The maximum intensity of tropical cyclones in axisymmetric numerical model simulations. *Mon. Wea. Rev.,* **137**, 1770-1789.

Dunion, J. P., 2011: Rewriting the climatology of the tropical North Atlantic and Caribbean sea atmosphere, *J. Climate*, **24**, 893-908.

Emanuel, K. A., 1986: An air-sea interaction study for tropical cyclones. Part I: Steady-state maintenance. J. Atmos. Sci., **43**, 585-604.

____, 1995: Sensitivity of tropical cyclones to surface exchange coefficients and a revised steady-state model incorporating eye dynamics. J. Atmos. Sci., **52**, 3969-3976.

Kossin, J. P. and W. H. Schubert, 2001: Mesovortices, polygonal flow patterns, and rapid pressure falls in hurricane-like vortices. *J. Atmos. Sci*., **58**, 2196-2209.

Nolan, D. S. and M. T. Montgomery, 2002: Nonhydrostatic, three-dimensional perturbations to balanced, hurricane-like vortices. Part I: Linearized formulation, stability, and evolution. *J. Atmos. Sci*., **59**, 2989-3020.

Rotunno, R., and K. A. Emanuel, 1987: An air-sea in- teraction theory for tropical cyclones. Part II: Evolutionary study using a nonhydrostatic axisymmetric numerical model. *J. Atmos. Sci.*, **44**, 542–561.

Rozoff, C. M., J. P. Kossin, W. H. Schubert, and P. J. Mulero, 2009: Internal control of hurricane intensity variability: The dual nature of potential intensity mixing. *J. Atmos. Sci.*, **66**, 133-147.

Schecter D. A., and M. T. Montgomery, 2007: Waves in a cloudy vortex, *J. Atmos. Sci*., **64**, 314-337.

Schubert, W. H., M. T. Montgomery, R. K. Taft, T. A. Guinn, S. R. Fulton, J. P. Kossin, and J. P. Edwards, 1999: Polygonal eyewalls, asymmetric eye contraction, and potential vorticity mixing in hurricanes. *J. Atmos. Sci.*, **56**, 1197–1223.